



Article

Jasmonate and Ethylene-Regulated Ethylene Response Factor 22 Promotes Lanolin-Induced Anthocyanin Biosynthesis in ‘Zaosu’ Pear (*Pyrus bretschneideri* Rehd.) Fruit

Ting Wu, Han-Ting Liu, Guang-Ping Zhao, Jun-Xing Song, Xiao-Li Wang, Cheng-Quan Yang, Rui Zhai, Zhi-Gang Wang *, Feng-Wang Ma and Ling-Fei Xu *

College of Horticulture, Northwest A&F University, Taicheng Road NO.3, Yangling 712100, Shaanxi Province, China; 18829351538@163.com (T.W.); hylht3598@163.com (H.-T.L.); zhaogp1996@nwfau.edu.cn (G.-P.Z.); JunxingSong@163.com (J.-X.S.); XiaoLiW365@163.com (X.-L.W.); cqyang@nwsuaf.edu.cn (C.-Q.Y.); zhongdishaonian@sina.com (R.Z.); fwm64@sina.com (F.-W.M.)

* Correspondence: wzhg001@163.com (Z.-G.W.); lingfxu2013@sina.com (L.-F.X.); Tel.: +86-029-15091443871 (Z.-G.W.); +86-029-87081023 (L.-F.X.)

Received: 3 January 2020; Accepted: 8 February 2020; Published: 11 February 2020



Abstract: Anthocyanin contributes to the coloration of pear fruit and enhances plant defenses. Members of the ethylene response factor (ERF) family play vital roles in hormone and stress signaling and are involved in anthocyanin biosynthesis. Here, *PbERF22* was identified from the lanolin-induced red fruit of ‘Zaosu’ pear (*Pyrus bretschneideri* Rehd.) using a comparative transcriptome analysis. Its expression level was up- and down-regulated by methyl jasmonate and 1-methylcyclopropene plus lanolin treatments, respectively, which indicated that *PbERF22* responded to the jasmonate- and ethylene-signaling pathways. In addition, transiently overexpressed *PbERF22* induced anthocyanin biosynthesis in ‘Zaosu’ fruit, and a quantitative PCR analysis further confirmed that *PbERF22* facilitated the expression of anthocyanin biosynthetic structural and regulatory genes. Moreover, a dual luciferase assay showed that *PbERF22* enhanced the activation effects of *PbMYB10* and *PbMYB10b* on the *PbUFGT* promoter. Therefore, *PbERF22* responds to jasmonate and ethylene signals and regulates anthocyanin biosynthesis. This provides a new perspective on the correlation between jasmonate–ethylene crosstalk and anthocyanin biosynthesis.

Keywords: pear; anthocyanin; *PbERF22*; MYB transcription factors; ethylene; jasmonate

1. Introduction

Anthocyanins, an important class of plant secondary metabolites, play important roles in plant growth and development and in resistance to environmental stresses [1]. The color affects fruit quality, and the formation of fruit pigments depends on anthocyanin synthesis during fruit growth and development. Moreover, in plants, accumulated anthocyanins enhance resistance to biotic and abiotic stresses, such as UV-B light damage [2], pathogen infection [3], wounding [4], and drought [5].

The anthocyanin biosynthetic pathway has been researched and illuminated in many species. A series of enzymes encoded by structural genes (*PAL*, *CHS*, *CHI*, *F3H*, *DFR*, *ANS*, and *UFGT*) are involved in anthocyanin biosynthesis, and these structural genes are co-regulated by the MBW transcription complex composed of myeloblastosis (MYB), basic helix-loop-helix proteins (bHLH), and WD40 proteins. In pear, flavonoid 3-O-glucosyltransferase (UFGT) is the key enzyme that determines the anthocyanin content in the fruit peel [6,7]. *MYB10.1* isolated from pear (*Pyrus pyrifolia* cv. Aoguan)

is similar to *MYB10*, and it interacts with bHLH3 to promote anthocyanin biosynthesis in pear [8]. In apple, *MdMYB1* is positively correlated with anthocyanin biosynthesis [9]. The overexpression of *MdMYB10* significantly enhances anthocyanin accumulation [10]. In *Prunus*, the overexpression of *MYB10.1/bHLH3* and *MYB10.3/bHLH3* increases the expression levels of *NtCHS*, *NtDFR*, and *NtUFGT* to promote anthocyanin synthesis [11]. In addition to the *MYB-bHLH-WD40* (MBW) complex, other transcription factors can coordinately regulate the expression of genes involved in anthocyanin synthesis. *Arabidopsis thaliana* *ZAT6* directly binds the promoters of *MYB12* and *MYB111* to activate the expression levels of genes involved in anthocyanin biosynthesis in plants treated with H₂O₂ [12]. *MdWRKY40* interacts with *MdMYB1* to promote wounding-induced anthocyanin biosynthesis in apple [13]. *PpHY5* directly binds to the promoter regions of *PpCHS*, *PpDFR*, *PpANS*, and *PpMYB10*, thereby promoting anthocyanin accumulation [14].

The ethylene response factor (ERF) family, belonging to the AP2/ERF transcription factor family, plays an essential role in plant growth, and its members can be stimulated by ethylene, jasmonate, abscisic acid, and auxin. They are involved in regulating various processes in plants, such as defense and stress responses [15]. *MdERF3* interacts with *MdMYC2* to activate *MdACS1* transcription, thereby participating in jasmonate- and ethylene-mediated apple fruit ripening [16]. ERF1 responses to ethylene and jasmonic acid play important roles in ethylene/jasmonic acid-dependent defense responses [17]. The ERF proteins enhance plant defense systems by activating a pathogen-inducible plant defense gene, PDF1.2 [18]. Moreover, *ERF* genes appear to regulate anthocyanin synthesis in various species. Under drought-stress conditions, the interaction between *MdERF38* and *MdMYB1* promotes anthocyanin biosynthesis [19]. *MdERF1B* regulates anthocyanin biosynthesis by interacting with *MdMYB9* and *MdMYB11* in apple [20]. The down-regulation of *JcERF035* accelerates anthocyanin accumulation under low-phosphate conditions in *Arabidopsis* [21]. *PyERF3* interacts with *MYB114* and forms a new complex with bHLH3 to co-regulate anthocyanin biosynthesis [22]. *Pp4ERF24* and *Pp12ERF96* are involved in fruit coloration and the anthocyanin synthesis induced by blue light in pear [23].

Lanolin, a complex mixture, consisting of esters of sterols, triterpene alcohols, esters of aliphatic alcohols, and mono-hydroxyesters of sterols, triterpenes, and aliphatic alcohols, has wide applications not only in chemical and medicinal industries [24], but also in plant research. It has been used extensively in plant research as a carrier for plant growth regulators [25] and as a main component of fungicides [26]. The earliest research on the use of lanolin in plants was carried out by Laibech et al. [27,28]. It has since been used as a carrier for plant growth regulators in many studies on the physiological responses of plants, such as during parthenocarpy [29], fruit development [30], and the rooting of cuttings [31], with pure lanolin treatments serving as negative controls in these studies. Lanolin alone has no significant physiological effects on some plant tissues, such as roots [32], stems [33], leaves [34], and flowers [35]. However, lanolin can affect other plant tissues sometimes. Applications of lanolin paste influence periderm development and tissue morphology in the rinds of melon fruits [36], and lanolin alone promotes shoot initiation from the axillary buds on the laterals of pruned kiwifruit vines [37].

In this study, we found an interesting phenomenon: lanolin was used on the fruit skin to cause the red coloration of the 'Zaosu' pear fruit. We further investigated the mechanisms of the skin coloration in pear and the anthocyanin biosynthetic pathway induced by this substance. *PbERF22*, as the candidate gene, was screened from RNA sequencing (RNA-Seq) data. We investigated its relationships with the two hormones jasmonate and ethylene and further verified the role of *PbERF22* in anthocyanin biosynthesis. The overexpression of *PbERF22* in pear confirmed the mechanism by which *PbERF22* regulates anthocyanin accumulation, and a dual luciferase (LUC) assay revealed that *PbERF22* enhances *PbUFGT* promoter activity. *PbERF22* may regulate anthocyanin biosynthesis by enhancing the activation effects of *PbMYB10* and *PbMYB10b* on the *PbUFGT* promoter. These studies provide a new perspective on the potential mechanisms of anthocyanin biosynthesis in green-skinned pear.

2. Materials and Methods

2.1. Plant Materials and Treatments

The experiment was carried out on a plantation in Wugong, Shaanxi Province, China, in May 2018. In total, 30 'Zaosu' fruit skins were coated with a thin layer of anhydrous lanolin (Xi'an Tianzheng Pharmaceutical Accessories Co. LTD', Xian, China; CAS: 8006-54-0) at 60 days after full bloom (DAFB), and untreated 'Zaosu' fruit were used as controls. Treated and untreated fruits were harvested after 10 and 20 days of normal growth. They were immediately transported to the laboratory on the same day. The lanolin remaining on the peel was removed with 75% alcohol before the skin was peeled off. The peels of five fruit were treated as a biological replicate. The peels of the fruit were peeled off. All the tissues were analyzed using three biological replicates. Isolated fruit peels were immediately frozen in liquid nitrogen and then stored at $-80\text{ }^{\circ}\text{C}$ for further use.

The 1-methylcyclopropene (1-MCP; an ethylene antagonist; Rohm & Haas, Philadelphia, Pennsylvania, PH, USA) was applied to fruit using the method described by Freiman et al. [38]. In June 2019, the 'Zaosu' pear fruit from the plantation in Wugong, Shaanxi Province, China, were treated at 90 DAFB with 1-MCP. Each fruit was wrapped in a plastic bag (low-density polyethylene, 16 cm \times 26 cm, 60- μm thick). Before sealing the bag, approximately 80 mg/L 1-MCP was released into the bag. The bag was removed after 24 h. Bagged untreated fruit served as the controls. Then, half of the untreated and 1-MCP-treated fruits were coated with lanolin, while the remaining half were not treated. After 10 days, all the fruit was harvested. Each treatment contained three biological replicates, each including five fruit.

A total of 100 'Zaosu' fruit were obtained 100 DAFB from an orchard in Meixian, Shaanxi Province, China, in July 2019, and they were immediately transported to the laboratory. The collected fruit was divided into two groups; one group was treated with water, and the other was treated by soaking in 2 mmol/L methyl jasmonate (MeJA; Sigma-Aldrich, Sigma-Aldrich, St Louis, MO, USA) for 5 min at room temperature, as described by Ma et al. [39]. The two fruit groups were dried and then placed at room temperature for 8 days. They were sampled every 4 days. The peels of five fruit served as a biological replicate. The fruit peels were peeled off. All the tissues were analyzed using three biological replicates. Isolated fruit peels were immediately frozen in liquid nitrogen and then stored at $-80\text{ }^{\circ}\text{C}$ for further use.

2.2. Measurement of the Anthocyanin Contents

The total anthocyanin extraction was performed using the slightly modified method of Giusti and Wrolstad (2001) [40]. Briefly, the peel tissue was quickly ground into a powder in liquid nitrogen, 0.2 g was weighed, and 2 mL of the 1% HCL-methanol solution was added. Next, the specific extraction methods and anthocyanin content calculations were performed using the method of Wang et al. [41]. The absorbance levels of extracts at 520 nm and 700 nm were determined using a UV-Visible spectrophotometer (UV-1700, Kyoto, Japan). The total anthocyanin content is presented as mg/100 g fresh weight. The value for each sample is expressed as the means of three independent biological replicates.

2.3. RNA Extraction and cDNA Synthesis

Fruit from each sampling point were divided into three groups, with each group containing five fruit. The peels in each group were evenly mixed for the total RNA extraction and used as one biological replication. The total RNA extraction was carried out using an RNAPrep Pure Plant Kit (TIANGEN, Beijing, China) in accordance with the manufacturer's instructions. The RNA concentration and quality were tested using a UV-Visible spectrophotometer (UV-1700, Kyoto, Japan). The first-strand cDNA was synthesized from 1 μg of total RNA using a PrimeScript RT reagent kit with gDNA Eraser (TaKaRa, Dalian, China) and used for quantitative real-time PCR assays.

2.4. Library Construction and Transcriptome Analysis

Samples of lanolin-treated and untreated control 'Zaosu' fruits peel from 10 and 20 days after treatment were used to construct RNA-Seq libraries. The 12 RNA-Seq libraries constructed were as follows: Untreated-10 (10-day control), Untreated-20 (20-day control), Lanolin-10 (10 days after lanolin-treatment), and Lanolin-20 (20 days after lanolin-treatment), each with three biological replicates. All the libraries were obtained using the following steps: total RNA detection, mRNA enrichment, double-stranded cDNA synthesis, purified double-stranded cDNA' terminal repair, AMPure XP bead-based fragment selection, PCR-amplification enrichment, and quality control analyses.

The libraries were used to carry out Illumina HiSeq sequencing. To ensure the quality of the RNA-sequencing information analysis, raw reads were filtered to select clean reads and eliminate low-quality reads with adapters. The clean reads obtained were used in the subsequent statistical analysis. The gene expression levels were estimated using the expected number of fragments per kilobase of transcript sequence per millions base pairs sequenced method. The genes that met the screening standards of $\text{padj} < 0.05$ and $|\log_2(\text{ratio})| > 1$ were defined as differentially expressed genes (DEGs). The pathway enrichment analyses of Kyoto Encyclopedia of Genes and Genomes (KEGG) were conducted using the website platform (www.genome.jp/kegg/).

2.5. Quantitative Real-Time PCR Validation

The qRT-PCR reactions contained SYBR Premix Ex Taq II (TaKaRa, Dalian, China) in accordance with the manufacturer's instructions and were performed on an Icyler iQ5 (Bio-Rad, Berkeley, CA, USA). Three biological replications were performed for each sample, and three technical replications were performed for each biological sample. The actin gene was used as the internal reference gene. Relative expression levels were measured using the cycle threshold (Ct) $2^{-\Delta\Delta\text{Ct}}$ method. The primers for all the genes investigated are listed in Table S1.

2.6. Transient Overexpression Experiments

For *Agrobacterium*-mediated transient expression, the full-length complete coding DNA sequences (CDS) of *PbERF22* (XM_009358931) were amplified and inserted individually into the vector pGreenII 62-SK to use for overexpression in 'Zaosu' fruit. The negative controls were infiltrated with *Agrobacterium* containing the pGreenII 62-SK-GUS and used for GUS staining. The GUS staining was performed as described by Zhai et al. [42]. All the constructs were transformed into *Agrobacterium* strain EHA105. The *Agrobacterium* EHA105 lines were incubated and resuspended to an OD_{600} of 0.6 in infiltration buffer containing MgCl_2 , MES, and acetosyringone. The fruit infiltration method used was as described by Zhai et al. [43]. At 3 d after injection, the peels around the injection sites were used for qRT-PCR. At 7 d after injection, the same sites were used for anthocyanin content and phenotype analyses. The primers for the constructed vectors are listed in Table S2.

2.7. Dual Luciferase Assay

The promoter region of *PbUFGT* was amplified by PCR using specific primers. The PCR product was fused with the Firefly luciferase (*LUC*) reporter gene in the pGreen II 0800-LUC vector to obtain *PbUFGT* pro-LUC. The effector vectors of pGreen II 62-SK-*PbERF22*, pGreen II 62-SK-*PbbHLH3*, pGreen II 62-SK-*PbMYB10*, and -*PbMYB10b* were also constructed. All the constructed vectors were transformed into *Agrobacterium* strain GV3101 (psoup). They were transiently expressed in the agroinfiltrated leaves of *Nicotiana benthamiana*, and a subsequent dual LUC assay was performed. LUC and Renilla (REN) luciferase activities were assayed using the dual LUC assay kit (Promega, Madison, WI, USA), and the LUC/REN activity analysis was performed as described previously by An et al. [44]. Three assay measurements were performed for each construct. The primers for all the constructed vectors are listed in Table S2.

2.8. Statistical Analyses

Statistical analyses of data were conducted using SPSS 23.0 software (SPSS, Chicago, IL, USA). Significant difference analyses were calculated using a one-way ANOVA test. The significant correlation analyses of gene transcription levels were performed using Pearson's correlation analysis method based on $p \leq 0.05$. Each value represents the mean \pm standard deviation of three independent biological replicates.

3. Results

3.1. Changes in Coloration and Expression Levels of Anthocyanin Biosynthesis-Related Genes in Lanolin-Treated 'Zaosu' Pear

On the 10th day after receiving the lanolin treatment, the color of 'Zaosu' fruit peels were significantly redder than those of fruit growing under normal conditions (Figure 1a). The anthocyanin content after the lanolin treatment was significantly higher than that the control, which is consistent with the observed phenotype (Figure 1b). Moreover, the expression levels of the anthocyanin biosynthetic regulatory genes, *PbMYB10* and *PbMYB10b*, and the structural genes, *PbUFGT*, *PbANS*, and *PbDFR* significantly increased (Figure 1c). These results indicated that the lanolin treatment induced the red coloration of green-skinned 'Zaosu' pear fruit and promoted anthocyanin accumulation by up-regulating the expression levels of related structural and regulatory genes.

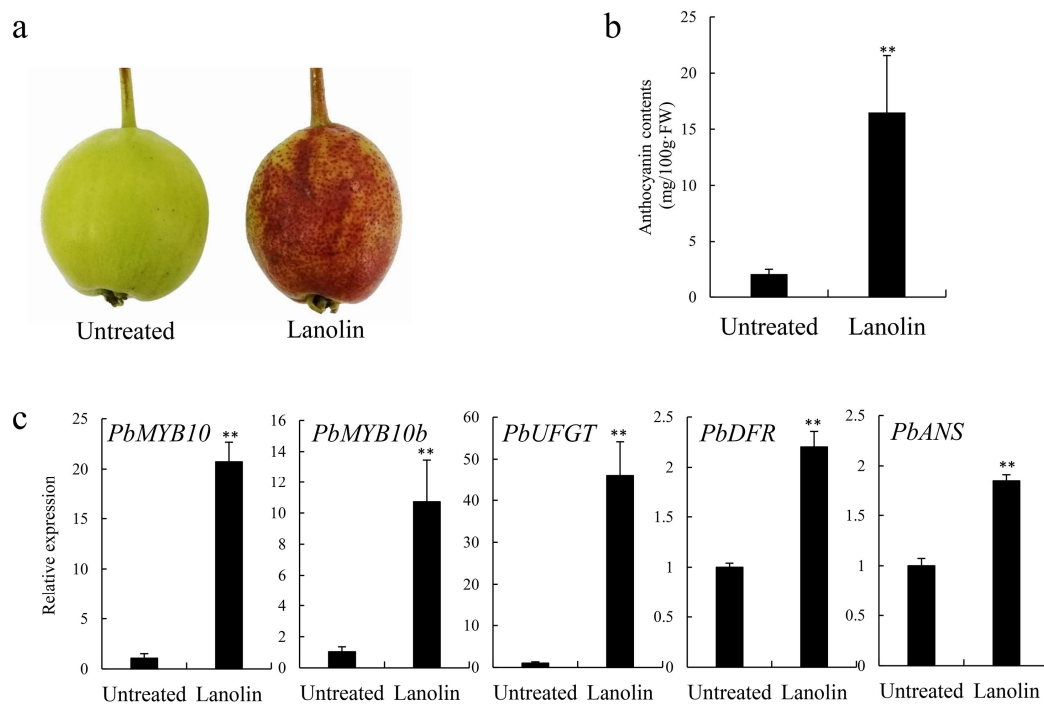


Figure 1. Anthocyanin biosynthesis was induced by a lanolin treatment in 'Zaosu' pear fruit at 10 d after treatment. (a) For untreated control and lanolin-treated 'Zaosu' fruit phenotypes of peels at 10 days after treatment; (b) total anthocyanin contents; and (c) expression levels of anthocyanin biosynthetic structural and regulatory genes were determined. ** indicates significant differences at $p < 0.01$. All the data are means \pm SDs of three biological replicates.

3.2. Transcriptome Data Analysis

To further investigate the lanolin-induced anthocyanin biosynthetic pathway, the untreated control and lanolin-treated 'Zaosu' fruit peels were subjected to an RNA-Seq analysis. To reduce the influence of the fruit development process and other factors, we selected two stages of lanolin-induced 'Zaosu'

fruit coloration for the transcriptome analysis. This allowed us to quickly screen out the differentially expressed genes (DEGs) related to coloration. At 10 and 20 days after the lanolin treatment compared with the untreated control, 1351 and 2687 genes, having absolute values of \log_2 (fold change) ≥ 2 , were identified as lanolin-induced DEGs, respectively. Among the DEGs, 748 were identified in both stages. Therefore, these 748 DEGs were selected as being potentially associated with the lanolin-induced coloration of 'Zaosu' fruit and were subjected to further functional analyses (Figure 2a). The KEGG enrichment analysis indicated that in addition to the metabolic pathways, other biological pathways produced extremely high P-values in this analysis. These indicated that the DEGs were significantly enriched in the biosynthesis of secondary metabolites, flavonoids, amino sugars, and nucleotide sugars, as well as plant hormone signal transduction and plant–pathogen interactions (Figure 2b). Moreover, a gene ontology (GO) annotation and enrichment analysis showed that the genes in the biological process group were mainly concentrated in the oxidation–reduction process, which is the molecular function term primarily concerned with oxidoreductase activity (Figure S1). These analyses indicated that multiple physiological mechanisms were involved in lanolin-induced anthocyanin biosynthesis. Here, the significant enrichment of DEGs in plant hormone signal transduction is of interest.

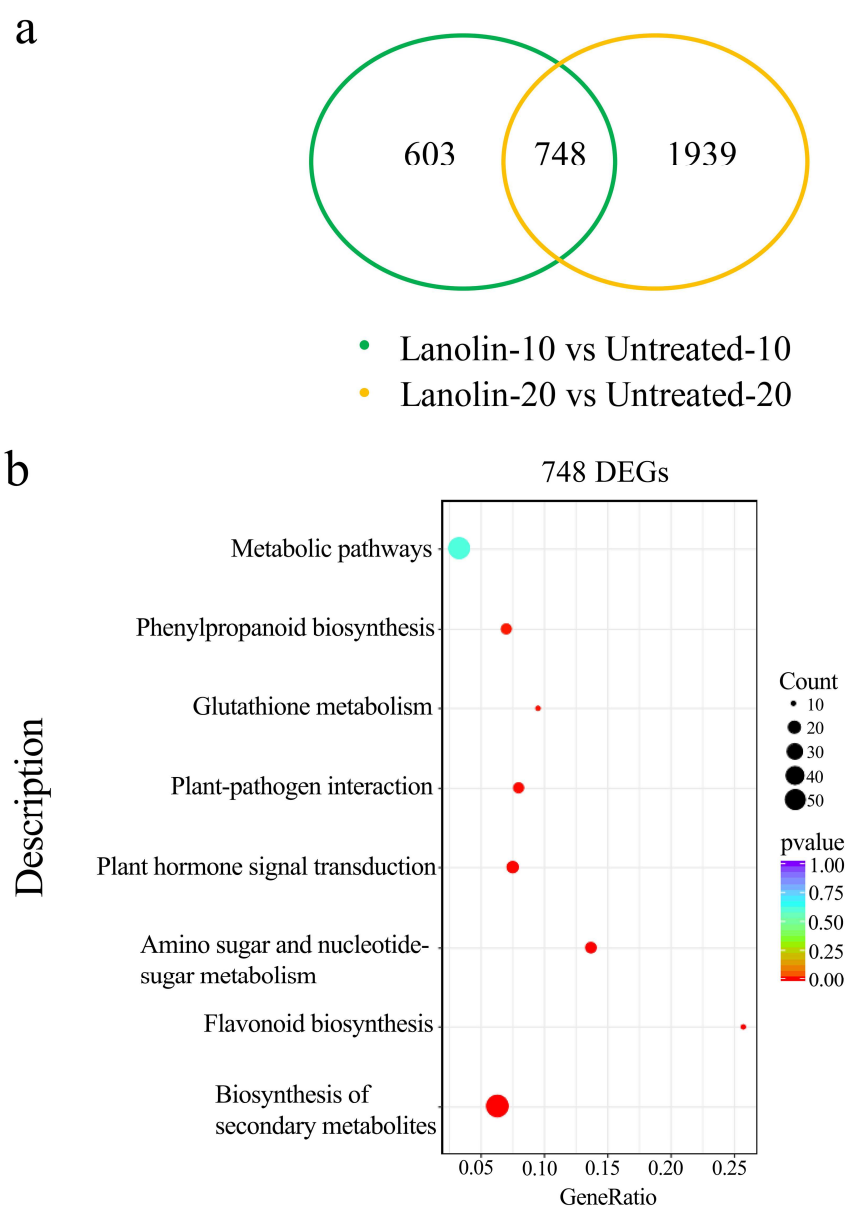


Figure 2. RNA-Seq analysis of untreated control and lanolin-treated 'Zaosu' pear fruit peels. (a) Venn

diagram of the numbers of differential expression genes (DEGs) between untreated and lanolin-treated fruit peels at 10 and 20 days after treatment. (b) The Kyoto Encyclopedia of Genes and Genomes (KEGG) enrichment analysis of 748 DEGs.

3.3. Lanolin-Induced Expression Levels of Jasmonate and Ethylene Synthesis-Related Genes

Based on the RNA-Seq analysis, we investigated the role of hormones in the lanolin-induced mechanism of anthocyanin biosynthesis. We found that the expression levels of the jasmonate synthetic genes *PbAOC*, *PbAOS*, *PbLOX*, and *PbOPR3* were significantly higher than those of the untreated control (Figure 3a). In addition, the expression levels of the ethylene synthetic genes *PbACO1* and *PbACS1* increased significantly in lanolin-induced pear compared with those in untreated controls (Figure 3b). Thus, the jasmonate and ethylene pathways are potentially involved in lanolin-induced anthocyanin biosynthesis.

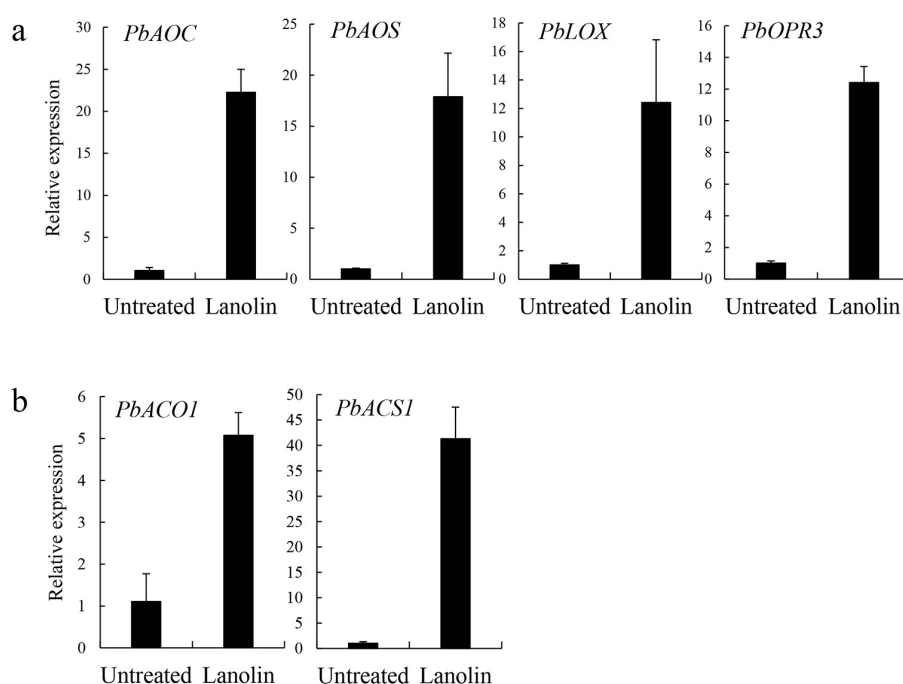


Figure 3. The expression analysis of jasmonate- and ethylene synthesis-related genes. The expression levels of (a) jasmonate and (b) ethylene synthetic genes in lanolin-treated and untreated control ‘Zaosu’ pear fruit after 10 days of treatment. Data are means \pm SDs of three biological replicates.

3.4. Identification of *PbERF22* As a Candidate Gene Involved in Anthocyanin Biosynthesis

Since both jasmonate and ethylene were involved in lanolin-induced responses, we focused on a class of *ERF* genes in the transcriptome data. *PbERF22*, a candidate gene, was screened from the RNA-Seq data. A qRT-PCR analysis showed that the expression level of *PbERF22* was significantly higher after the lanolin treatment compared with the control (Figure 4a), which was consistent with its transcript abundance in the transcriptome data.

Furthermore, ‘Zaosu’ pear fruit were harvested at 100 DAFB, treated with 2 mmol/L MeJA, and stored at room temperature for 8 d. The *PbERF22* expression level increased significantly in MeJA-treated fruit compared with in controls (Figure 4b). Additionally, ‘Zaosu’ pear fruit at 90 DAFB were treated with 1-MCP, lanolin, or with 1-MCP followed by lanolin, and then, they were harvested 10 d later. The phenotype of pear fruit treated with lanolin was almost the same as those receiving the co-treatment of 1-MCP and lanolin (Figure 4c), which indicated that ethylene might not be a key factor, but only a participant, in lanolin-induced coloration. The expression levels of *PbACO1*, *PbACS1*,

and *PbERF22* increased after the lanolin treatment. The expression levels of *PbACO1* and *PbACS1* increased significantly after the co-treatment of 1-MCP and lanolin compared with the 1-MCP treatment, and their expression levels decreased significantly compared with those in the lanolin treatment. This result demonstrated that 1-MCP successfully inhibited ethylene synthesis in the co-treated fruit. Compared with in the lanolin treatment, the expression level of *PbERF22* was significantly reduced in fruit co-treated with 1-MCP and lanolin (Figure 4d). These results indicated that the expression level of *PbERF22* was influenced by jasmonic acid and ethylene.

We analyzed the correlation between *PbERF22* and anthocyanin biosynthesis-related genes based on the transcriptional abundance levels of genes in the transcriptome data. *PbERF22* was significantly correlated with *PbMYB10* and *PbUFGT*, having correlation coefficients of 0.734 and 0.800, respectively (Table 1). In addition, the *PbERF22* expression levels during different developmental stages of several red-skinned pears were notably higher than those in ‘Zaosu’ pear (Figure S2a). Therefore, we believed that *PbERF22* was related to lanolin-induced anthocyanin biosynthesis.

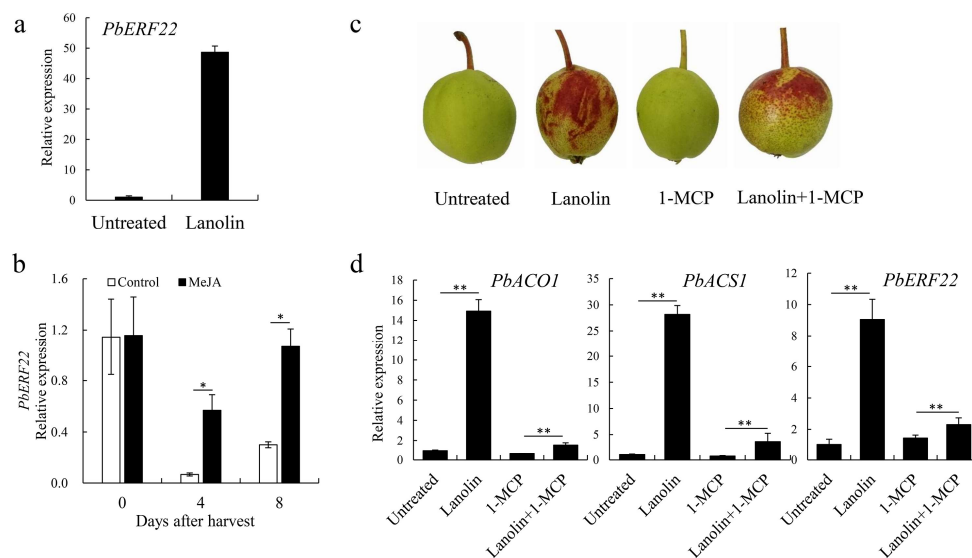


Figure 4. *PbERF22* responded to jasmonate and ethylene and was selected as a candidate gene related to anthocyanin biosynthesis. (a) Quantitative real-time PCR analysis of *PbERF22* expression levels in lanolin-treated and untreated control ‘Zaosu’ fruit; (b) *PbERF22* expression levels after methyl jasmonate (MeJA) and water (control) treatments. ‘Zaosu’ pear fruit were harvested at 100 days after full bloom (DAFB), treated independently with 2 mmol/L MeJA and water, and then stored at room temperature for 8 d; (c) The phenotypes of ‘Zaosu’ pear and treated with lanolin, 1-methylcyclopropene (1-MCP; an ethylene antagonist), or with lanolin followed by 1-MCP. Untreated pear served as the controls; (d) The expression levels of *PbACO1*, *PbACS1*, and *PbERF22* in the above treated pear fruit. In (c) and (d), fruit on the ‘Zaosu’ fruit tree were treated at 90 DAFB with 1-MCP or lanolin, or with 1-MCP followed by lanolin and then obtained 10 days after treatment. * indicates significant differences at $p < 0.05$, ** indicates significant differences at $p < 0.01$. Error bars for the data represent \pm SDs of three biological replicates.

Table 1. Correlation analysis between *PbERF22* and anthocyanin biosynthesis-related genes.

Correlation of Factor	<i>PbERF22</i>	<i>PbMYB10</i>	<i>PbMYB10b</i>	<i>PbUFGT</i>	<i>PbDFR</i>	<i>PbANS</i>
<i>PbERF22</i>	1	0.734 **	0.565	0.800 **	0.456	0.121
<i>PbMYB10</i>		1	0.469	0.749 **	0.399	0.581 *
<i>PbMYB10b</i>			1	0.769 **	0.693 *	−0.159
<i>PbUFGT</i>				1	0.689 *	−0.066
<i>PbDFR</i>					1	−0.114
<i>PbANS</i>						1

*: Correlation is significant at the 0.05 level ($p < 0.05$, two tailed); **: Correlation is significant at the 0.01 level ($p < 0.01$, two tailed).

3.5. Transient Overexpression of *PbERF22* in ‘Zaosu’ Pear

To verify *PbERF22*'s function in anthocyanin biosynthesis, the transient transformation of *PbERF22* was performed in young ‘Zaosu’ pear (Figure 5a; Figure S3). The overexpression of *PbERF22* resulted in the anthocyanin contents significantly increasing when compared with control fruit (Figure 5b). Compared with the empty vector, the significant up-regulation of *PbERF22* in fruit indicated that the transient transformation experiment was successful. The overexpression of *PbERF22* significantly up-regulated the expression levels of structural genes *PbCHS*, *PbDFR*, *PbANS*, and *PbUFGT* compared with their levels in controls (Figure 5c). Moreover, the expression levels of regulatory genes *PbMYB10*, *PbMYB10b*, and *PbbHLH3* were also up-regulated significantly (Figure 5d). Therefore, *PbERF22* promoted anthocyanin accumulation by up-regulating the expression levels of structural and regulatory genes.

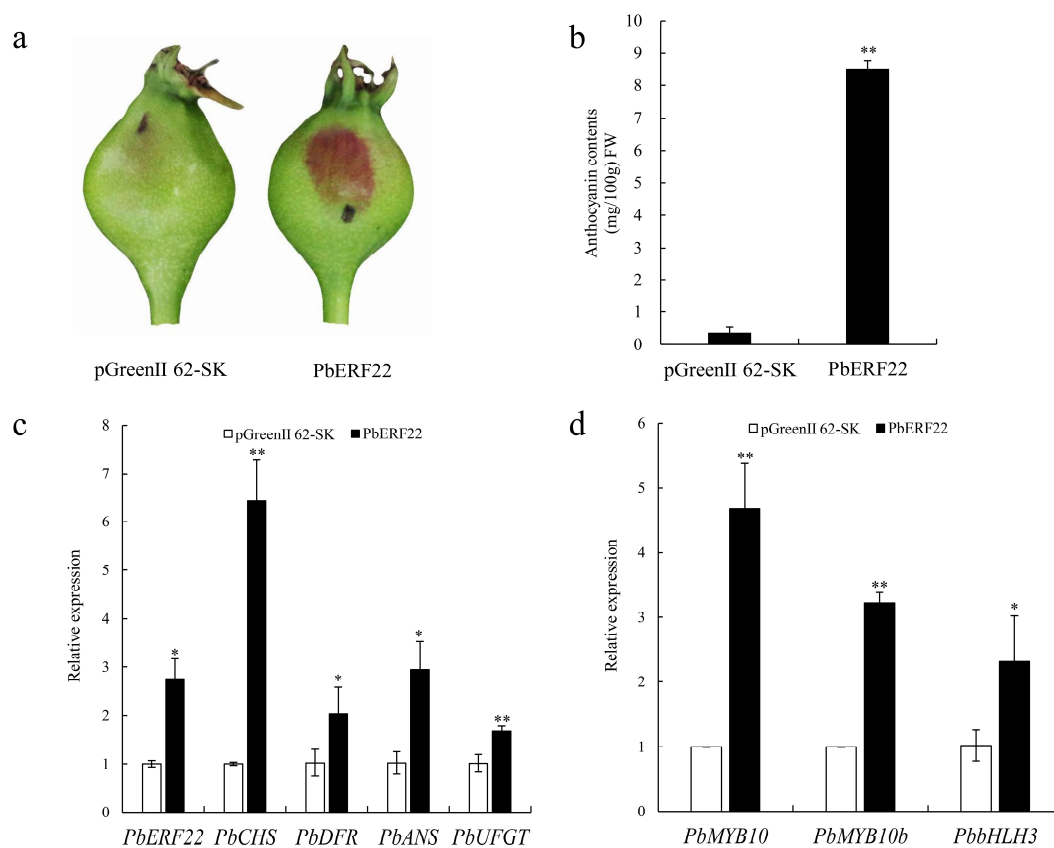


Figure 5. Transient transformation assays verifying *PbERF22*'s function in the coloration of ‘Zaosu’ fruit peel. (a) The phenotype of the ‘Zaosu’ pear 7 d after overexpressing *PbERF22* and the empty vector (pGreenII 62-SK), which were introduced by infiltration; (b) Measurements of anthocyanin contents in the injection regions of fruit peel; (c) qRT-PCR analysis of the expression levels of anthocyanin structural genes after infiltration; (d) The expression levels of anthocyanin regulatory genes. * indicates significant differences at $p < 0.05$, ** indicates significant differences at $p < 0.01$. Error bars represent \pm SDs of three biological replicates.

3.6. Effects of *PbERF22* on *PbUFGT* Promoter Activity

To verify how *PbERF22* regulates the expression levels of anthocyanin biosynthesis-related genes, we performed a dual LUC assay in tobacco leaves. *PbMYB10*, *PbMYB10b*, and *PbERF22* activated the promoter of *PbUFGT*. When *PbMYB10* or *PbMYB10b* was present, *PbERF22* enhanced the activation effects of *PbMYB10* and *PbMYB10b* on the *PbUFGT* promoter. Moreover, *PbERF22* enhanced the activity of the *PbUFGT* promoter in the presence of *PbMYB10* or *PbMYB10b* and *PbbHLH3*. Interestingly,

compared with the co-transformation of *PbMYB10b* and *PbERF22*, the co-transformation of *PbERF22* and *PbMYB10* had a significantly greater activation effect on the *PbUFGT* promoter. Therefore, we believe that *PbERF22* significantly enhances the activation effect of the complex *MYB10-bHLH3* or *MYB10b-bHLH3* on the *PbUFGT* promoter.

4. Discussion

4.1. Lanolin Promotes Anthocyanin Biosynthesis in ‘Zaosu’ Pear Fruit

Initially, we noticed that several green-skinned pear fruit turned red when treated with lanolin during fruit development (Figure S4). Next, we studied the lanolin-treated ‘Zaosu’ fruit and found that lanolin induced red coloration on the sunny side of the pear fruit.

Many studies, using various methods to investigate anthocyanin synthesis in fruit, have been published. In strawberry, the use of red and yellow plastic films significantly increases the anthocyanin contents [45]. In pomegranate, chitosan coating treatments followed by cold storage reduce the anthocyanin degradation rate in juice and pomegranate arils [46]. In red Chinese sand pears, bagging, UV-B/visible irradiation, and jasmonic acid treatments affect the expression levels of genes related to anthocyanin synthesis and accumulation [47]. Thus, most red-skinned fruits have been used in anthocyanin biosynthetic studies, while the green-skinned fruits have been used less. In this study, although the lanolin application to induce anthocyanin biosynthesis was unique in pear fruit, the lanolin treatment resulted in the red coloration of green-skin pear and altered the fruits’ appearance. Lanolin promoted anthocyanin biosynthesis by inducing the up-regulation of genes related to anthocyanin biosynthesis (Figure 1).

Many studies have shown that pure lanolin as negative controls, when applied to stems, leaves, and pedicels of plants [33,34,48], produces no significant physiological responses in these tissues because of its physical stability and chemical inertness. The cuttings of *Coleus* red were treated with diluted lanolin in greenhouses, its root formation is not affected [25]. However, a finding has shown that pure lanolin, when applied on chrysanthemum cuttings in summer, interferes with the rooting of cuttings [49]. These different effects of lanolin on the rooting of cuttings may be related to concentration of lanolin and environment of the treatment. In addition, lanolin affects pericarp development [36] and lateral bud germination [37]. In our study, anhydrous lanolin was applied to the fruit peel during fruit development, and this induced red coloration and physiological effects. Our preliminary study showed that lanolin induced red coloration because of the stimulation caused by lanolin itself rather than the temperature (Figure S5). Moreover, it caused physiological processes of flavonoid biosynthesis, plant hormone signal transduction, plant–pathogen interactions, and oxidation reduction (Figure 2; Figure S1). Therefore, we speculated that lanolin induced biological effects to plant tissues in some environments of treatment, and thus, it may not be an ideal negative control.

4.2. Lanolin Affects the Levels of Several Hormones in ‘Zaosu’ Pear Fruit

Plant hormones are important signal transducers in plant cells that respond to the external environment [50,51] and vital factors affecting anthocyanin biosynthesis [52–54]. The RNA-Seq analysis showed that DEGs were significantly enriched in plant hormone signal transduction (Figure 2b). Therefore, we measured the contents of several hormones in lanolin-treated ‘Zaosu’ pear fruit and found that the jasmonate contents were significantly increased and the abscisic acid contents were significantly decreased (Figure S6). Moreover, through a transcription factor family analysis, we found that ERFs were highly enriched (Figure S7), which caused us to speculate that the ethylene synthesis pathway had proceeded in lanolin-treated ‘Zaosu’ pear fruit.

A gene expression analysis further indicated that the jasmonate synthetic genes *PbAOC*, *PbAOS*, *PbLOX*, and *PbOPR3* and the ethylene synthetic genes *PbACS1* and *PbACO1* were significantly up-regulated (Figure 3). *PbAOC*, *PbAOS*, *PbLOX*, and *PbOPR3* are the key genes of the jasmonate synthetic pathway [55], while *PbACS1* and *PbACO1* are the key genes of the ethylene synthetic

pathway [56]. Although less ethylene production occurred in the 60 DAFB period of ‘Zaosu’ fruit, which might have led us to fail to measure ethylene production, the gene expression (Figure 3) and the transcription factor family (Figure S7) analyses indicated that ethylene production was also induced by lanolin. Therefore, we speculated that the crosstalk among multiple hormones was involved in lanolin-induced anthocyanin biosynthesis.

4.3. *PbERF22* Responses to Jasmonate and Ethylene and is Correlated with Anthocyanin Biosynthesis

Since lanolin treatments resulted in anthocyanin accumulation and jasmonate and ethylene changes, we focused on a class of *ERF* genes found in the transcriptome data. *ERF* genes respond to hormone signals, including those of jasmonate and ethylene [57]; *ERFs* are important components downstream in the ethylene signaling and response pathway, and they are involved in various ethylene-mediated responses [58,59]. *ERF* genes, such as *AtERF2* [60] and *BrERF72* [61], also positively respond to jasmonate signal-transduction pathways, and their expression levels are regulated synergistically by both ethylene and jasmonate. *ERF1* expression can be synergistically activated by jasmonate and ethylene to regulate defense-response genes [17]. In soybean, the jasmonic acid and ethylene treatments induce the expression of *GmERF3*, which has an important role in responses to biotic and abiotic stresses [62]. In tobacco, *JERF1* acts as a transcription factor in different signal-transduction pathways. It binds to the GCC box or dehydration-responsive element (DRE) sequence and responds to jasmonic acid, ethylene, and abscisic acid signals [63]. In this study, *PbERF22* was selected as a candidate gene based on an RNA-Seq data analysis. A qRT-PCR analysis showed that the *PbERF22* expression level was markedly up-regulated by lanolin (Figure 4a). Multiple cis-acting MeJA-responsive elements, including CGTCA and TGACG motifs [64], were identified by analyzing the *PbERF22* promoter sequence. Furthermore, we observed that the MeJA treatment promoted the *PbERF22* expression and that 1-MCP significantly reduced the *PbERF22* expression induced by lanolin. The expression patterns of *PbACS1* and *PbERF22* were highly similar, suggesting that *PbERF22* responds to jasmonate and ethylene (Figure 4).

In addition, *ERF* genes participate in the regulation of anthocyanin biosynthesis. The *AtERF4* and *AtERF8* double-mutant reduces the light-induced anthocyanin contents in Arabidopsis [65]. Under low-isoelectric point conditions, the anthocyanin contents in Arabidopsis lines that overexpress *JcERF035* decrease compared with the controls [21]. Here, a phylogenetic analysis found that *PbERF22* and *PyERF3* were clustered together in one clade (Figure S2b). *PyERF3* is involved in the regulation of anthocyanin biosynthesis in pears [22]. Furthermore, *PbERF22* was highly correlated with the expression levels of *PbMYB10* and *PbUFGT* (Table 1), and the *PbERF22* expression levels in several red-skinned pears were notably higher than those in ‘Zaosu’ pears (Figure S2a). Therefore, we speculated that *PbERF22* was involved in anthocyanin biosynthesis and was an important link between the jasmonate and/or ethylene hormone signals and anthocyanin biosynthesis.

4.4. Functional Validation of *PbERF22* in Anthocyanin Biosynthesis

To test the hypothesis that *PbERF22* is involved in anthocyanin biosynthesis, we investigated *PbERF22*'s function in anthocyanin biosynthesis. The overexpression of *PbERF22* promoted anthocyanin biosynthesis by up-regulating the expression levels of anthocyanin structural and regulatory genes in ‘Zaosu’ pear fruit (Figure 5). *UFGT*, a key gene in anthocyanin biosynthesis, is regulated by the MBW complex [7]. Transcription factors, including *ERFs*, are involved in the regulation of anthocyanin synthesis through interactions with the MBW complex. *ERF3* forms complexes with *MYB10* and *bHLH3* or *MYB114* plus *bHLH3* to enhance binding to the *UFGT* promoter and the co-regulation of anthocyanin biosynthesis [22]. *Pp4ERF24* and *Pp12ERF96* facilitate the *PpUFGT* activity level by enhancing interactions with *PpMYB114* and *PpbHLH3* [23]. *MYB10* and *MYB10b* positively regulate the expression levels of structural genes in the anthocyanin biosynthetic pathway in pear [43,66,67]. Therefore, in this study, we investigated whether *PbERF22* has effects on the ability of *PbMYB10* and *PbMYB10b* to activate the promoter of *PbUFGT*. We determined that *PbERF22* enhances the activation effect

of *PbMYB10* or *PbMYB10b* on the *PbUFGT* promoter. This result was similar to that of *PyERF3*, which enhances the transcriptional activities of *PyMYB10* and *PyMYB114* [22]. However, *PbERF22* showed more significant effects on the transactivation of *PbMYB10* or the complex of *PbMYB10* plus *PbbHLH3* on the *PbUFGT* promoter (Figure 6).

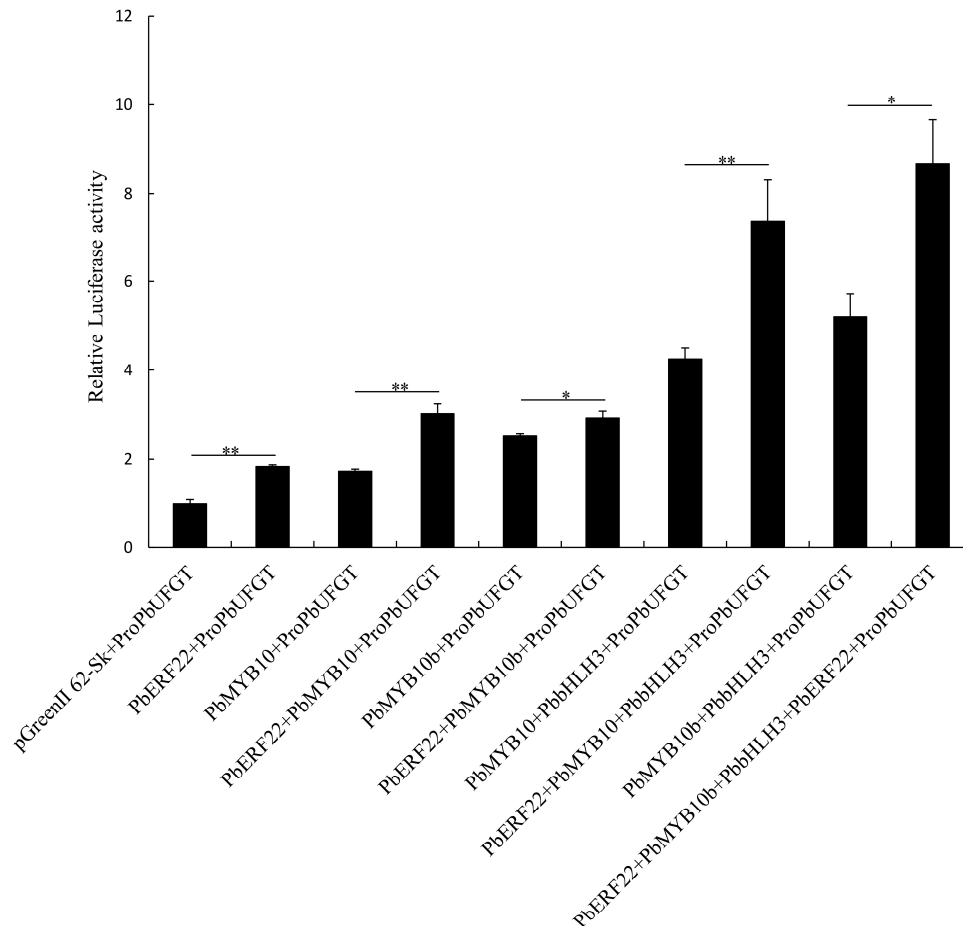


Figure 6. Dual luciferase (LUC) assay verifying that *PbMYB10*, *PbMYB10b*, and *PbbHLH3* co-transformed with *PbERF22* increased the *PbUFGT* promoter activity. The *PbUFGT* promoter activity is expressed as a ratio of LUC to Renilla (REN) activities. * indicates significant differences at $p < 0.05$, ** indicates significant differences at $p < 0.01$. Data are means \pm SEs of three biological replicates.

5. Conclusions

We found that lanolin can induce the red appearance of green-skinned pears, and that multiple pathways were involved in the complex coloring mechanism. *PbERF22* was confirmed to respond to jasmonate and ethylene signals and to promote anthocyanin biosynthesis by enhancing the activation effects of *MYB10* and *MYB10b*. We believe that *PbERF22* plays an important role in the interactions between hormones and anthocyanin biosynthesis. The lanolin-induced red phenomenon will allow us to gain insights into more mechanisms that influence the anthocyanin synthetic pathway in green-skinned pears.

Supplementary Materials: The following are available online at <http://www.mdpi.com/2218-273X/10/2/278/s1>, Figure S1: Gene ontology (GO) annotation and enrichment analysis of 748 DEGs, Figure S2: The expression levels of *PbERF22* in several red-skinned pear fruit, and Phylogenetic tree of ERFs from different species, Figure S3: The GUS-staining of ‘Zaosu’ fruit infiltrated with pGreenII 62-SK-GUS shown in vertical and horizontal planes, Figure S4: Phenotypes of several untreated and lanolin-treated green-skinned pears at the same developmental stages, Figure S5: ‘Zaosu’ fruit surface thermogram and the lanolin’s permeability analysis, Figure S6: Quantifications of phytohormones, Figure S7: Transcription factor family analysis at 10 (a) and 20 (b) d

of DEGs in lanolin-treated and untreated samples, Table S1: List of primers for qRT-PCR, Table S2: List of primers for vector construction.

Author Contributions: T.W. carried out the experiments and wrote the initial manuscript; Z.-G.W., R.Z., and L.-F.X. conceived the study; H.-T.L. performed the transient overexpression experiments, sorted, and analyzed the data; G.-P.Z., J.-X.S., and X.-L.W. performed the quantitative real-time PCR; G.-P.Z., collected and treated the plant materials; C.-Q.Y., Z.-G.W., R.Z., F.-W.M. and L.-F.X. amended and edited the manuscript. All authors have read and agreed to the published version of the manuscript.

Funding: This research was funded by the National Key Research and Development Program of China (No. 2019YFD1000104) and the National Natural Science Foundation of China (No. 31572086 and 31972372).

Acknowledgments: We thank Lesley Benyon, PhD, from Liwen Bianji, Edanz Group China (www.liwenbianji.cn/ac), for editing the English text of a draft of this manuscript.

Conflicts of Interest: The authors declare no conflict of interest.

References

1. Jia, Z.; Ma, P.; Bian, X.; Yang, Q.; Guo, X.; Xie, Y. Biosynthesis Metabolic pathway and molecular regulation of plants anthocyanin. *Acta Bot. Bor-Occid. Sin.* **2014**, *34*, 1496–1506.
2. Tsurunaga, Y.; Takahashi, T.; Katsube, T.; Kudo, A.; Kuramitsu, O.; Ishiwata, M.; Matsumoto, S. Effects of UV-B irradiation on the levels of anthocyanin, rutin and radical scavenging activity of buckwheat sprouts. *Food Chem.* **2013**, *141*, 552–556. [[CrossRef](#)] [[PubMed](#)]
3. Sun, X.; Zhou, T.; Wei, C.; Lan, W.; Zhao, Y.; Pan, Y.; Wu, V.C. Antibacterial effect and mechanism of anthocyanin rich Chinese wild blueberry extract on various foodborne pathogens. *Food Control* **2018**, *94*, 155–161. [[CrossRef](#)]
4. Reyes, L.F.; Cisneros, Z.L. Wounding stress increases the phenolic content and antioxidant capacity of purple-flesh potatoes (*Solanum tuberosum* L.). *J. Agric. Food Chem.* **2003**, *51*, 5296–5300. [[CrossRef](#)]
5. Cui, Z.; Bi, W.; Hao, X.; Li, P.; Duan, Y.; Walker, M.A.; Xu, Y.; Wang, Q. Drought stress enhances up-regulation of anthocyanin biosynthesis in grapevine leafroll-associated virus 3-Infected in vitro grapevine (*Vitis vinifera*) leaves. *Plant Dis.* **2017**, *101*, 1606–1615. [[CrossRef](#)]
6. Yang, Y.; Yao, G.; Yue, W.; Zhang, S.; Wu, J. Transcriptome profiling reveals differential gene expression in proanthocyanidin biosynthesis associated with red/green skin color mutant of pear (*Pyrus communis* L.). *Front. Plant Sci.* **2015**, *6*, 795. [[CrossRef](#)]
7. Zhai, R.; Liu, X.; Feng, W.; Chen, S.; Xu, L.; Wang, Z.; Zhang, J.; Li, P.; Ma, F.; Liu, J. Different biosynthesis patterns among flavonoid 3-glycosides with distinct effects on accumulation of other flavonoid metabolites in pears (*Pyrus bretschneideri* Rehd.). *PLoS ONE* **2014**, *9*, e91945. [[CrossRef](#)]
8. Feng, S.; Sun, S.; Chen, X.; Wu, S.; Wang, D.; Chen, X.; Zhang, P. PyMYB10 and PyMYB10.1 interact with bHLH to enhance anthocyanin accumulation in pears. *PLoS ONE* **2015**, *10*, e0142112. [[CrossRef](#)]
9. Takos, A.M.; Jaffe, F.W.; Jacob, S.R.; Bogs, J.; Robinson, S.P.; Walker, A.R. Light-induced expression of a MYB gene regulates anthocyanin biosynthesis in red apples. *Plant Physiol.* **2006**, *142*, 1216–1232. [[CrossRef](#)]
10. Espley, R.V.; Brendolise, C.; Chagne, D.; Kutty, A.S.; Green, S.; Volz, R.; Putterill, J.; Schouten, H.J.; Gardiner, S.E.; Hellens, R.P. Multiple repeats of a promoter segment causes transcription factor autoregulation in red apples. *Plant Cell* **2009**, *21*, 168–183. [[CrossRef](#)]
11. Rahim, M.A.; Busatto, N.; Trainotti, L. Regulation of anthocyanin biosynthesis in peach fruits. *Planta* **2014**, *240*, 913–929. [[CrossRef](#)] [[PubMed](#)]
12. Shi, H.; Zhang, S.; Lin, D.; Wei, Y.; Yan, Y.; Liu, G.; Reiter, R.; Chan, Z. Zinc finger of Arabidopsis thaliana 6 is involved in melatonin-mediated auxin signaling through interacting INDETERMINATE DOMAIN15 and INDOLE-3-ACETIC ACID 17. *J. Pineal Res.* **2018**, *65*, e12494. [[CrossRef](#)] [[PubMed](#)]
13. An, J.; Zhang, X.; You, C.; Bi, S.; Wang, X.; Hao, Y. MdWRKY40 promotes wounding-induced anthocyanin biosynthesis in association with MdMYB1 and undergoes MdbT2-mediated degradation. *New Phytol.* **2019**, *224*, 380–395. [[CrossRef](#)] [[PubMed](#)]
14. Tao, R.; Bai, S.; Ni, J.; Yang, Q.; Zhao, Y.; Teng, Y. The blue light signal transduction pathway is involved in anthocyanin accumulation in 'Red Zaosu' pear. *Planta* **2018**, *248*, 37–48. [[CrossRef](#)]
15. Gu, C.; Guo, Z.; Hao, P.; Wang, G.; Jin, Z.; Zhang, S. Multiple regulatory roles of AP2/ERF transcription factor in angiosperm. *Bot. Stud.* **2017**, *58*, 6. [[CrossRef](#)]

16. Li, T.; Xu, Y.; Zhang, L.; Ji, Y.; Tan, D.; Yuan, H.; Wang, A. The jasmonate-activated transcription factor MdMYC2 regulates ethylene response factor and ethylene biosynthetic genes to promote ethylene biosynthesis during apple fruit ripening. *Plant Cell* **2017**, *29*, 1316–1334. [[CrossRef](#)]
17. Lorenzo, O.; Piqueras, R.; Sánchez-serrano, J.J.; Solano, R. ETHYLENE RESPONSE FACTOR1 integrates signals from ethylene and jasmonate pathways in plant defense. *Plant Cell* **2003**, *15*, 165–178. [[CrossRef](#)]
18. Maruyama, Y.; Yamoto, N.; Suzuki, Y.; Chiba, Y.; Yamazaki, K.; Sato, T.; Yamaguchi, J. The Arabidopsis transcriptional repressor ERF9 participates in resistance against necrotrophic fungi. *Plant Sci.* **2013**, *213*, 79–87. [[CrossRef](#)]
19. An, J.; Zhang, X.; Bi, S.; You, C.; Wang, X.; Hao, Y. The ERF transcription factor MdERF38 promotes drought stress-induced anthocyanin biosynthesis in apple. *Plant J.* **2019**, *101*, 573–589. [[CrossRef](#)]
20. Zhang, J.; Xu, H.; Wang, N.; Jiang, S.; Fang, H.; Zhang, Z.; Yang, G.; Wang, Y.; Su, M.; Xu, L. The ethylene response factor MdERF1B regulates anthocyanin and proanthocyanidin biosynthesis in apple. *Plant Mol. Biol.* **2018**, *98*, 205–218. [[CrossRef](#)]
21. Chen, Y.; Wu, P.; Zhao, Q.; Tang, Y.; Chen, Y.; Li, M.; Jiang, H.; Wu, G. Overexpression of a phosphate starvation response AP2/ERF gene from physic nut in Arabidopsis alters root morphological traits and phosphate starvation-induced anthocyanin accumulation. *Front. Plant Sci.* **2018**, *9*, 1186. [[CrossRef](#)] [[PubMed](#)]
22. Yao, G.; Ming, M.; Allan, A.C.; Gu, C.; Li, L.; Wu, X.; Wang, R.; Chang, Y.; Qi, K.; Zhang, S.; et al. Map-based cloning of the pear gene MYB114 identifies an interaction with other transcription factors to coordinately regulate fruit anthocyanin biosynthesis. *Plant J.* **2017**, *92*, 437–451. [[CrossRef](#)] [[PubMed](#)]
23. Ni, J.; Bai, S.; Zhao, Y.; Qian, M.; Tao, R.; Yin, L.; Gao, L.; Teng, Y. Ethylene response factors Pp4ERF24 and Pp12ERF96 regulate blue light-induced anthocyanin biosynthesis in ‘Red Zaosu’ pear fruits by interacting with MYB114. *Plant Mol. Biol.* **2018**, *99*, 66–78. [[CrossRef](#)] [[PubMed](#)]
24. Schlossman, M.; McCarthy, J. Lanolin and its derivatives. *JAOCs* **1978**, *55*, 447–450. [[CrossRef](#)]
25. Fischnich, O. Über den einfluss von β -Indolylessigsäure auf die blattbewegungen und die adventivwurzelbildung von Coleus. *Planta* **1935**, *24*, 552–583. [[CrossRef](#)]
26. Castillo, F.; Daniel, H.; Gabriel, G.; Mendez, M.; Rodriguez, R.; Reyes, A.; Aguilar, C.N. In vitro antifungal activity of plant extracts obtained with alternative organic solvents against Rhizoctonia solani Kühn. *Ind. Crop. Prod.* **2010**, *32*, 324–328. [[CrossRef](#)]
27. Laibach, F.; Kornmann, P. Zur Frage des Wuchsstofftransportes in der Haferkoleoptile. *Planta* **1933**, *21*, 396–418. [[CrossRef](#)]
28. Laibach, F.; Mai, G.; Müller, A. Über ein Zellteilungshormon. *Naturwissenschaften* **1934**, *22*, 288. [[CrossRef](#)]
29. Hikosaka, S.; Sugiyama, N. Effects of exogenous plant growth regulators on yield, fruit growth, and concentration of endogenous hormones in gynoecious parthenocarpic cucumber (*Cucumis sativus* L.). *Horticult. J.* **2015**, *84*, 342–349. [[CrossRef](#)]
30. Zhang, C.X.; Whiting, M.D. Improving ‘Bing’ sweet cherry fruit quality with plant growth regulators. *Sci. Hortic.* **2011**, *127*, 341–346. [[CrossRef](#)]
31. Cooper, W.C. Hormones in relation to root formation on stem cuttings. *Plant Physiol.* **1935**, *10*, 789–794. [[CrossRef](#)] [[PubMed](#)]
32. McDavid, C.R.; Sagar, G.R.; Marshall, C. The effect of auxin from shoot on root development in *Pisum Sativum* L. *New Phytol.* **1972**, *71*, 1027–1032. [[CrossRef](#)]
33. Hao, B.Z.; Wu, J.L. Laticifer differentiation in Hevea brasiliensis: Induction by exogenous jasmonic acid and linolenic acid. *Ann. Bot.* **2000**, *85*, 37–43. [[CrossRef](#)]
34. Kost, C.; Heil, M. Herbivore-induced plant volatiles induce an indirect defence in neighbouring plants. *J. Ecol.* **2006**, *94*, 619–628. [[CrossRef](#)]
35. Zuniga-Mayo, V.M.; Banos-Bayardo, C.R.; Diaz-Ramirez, D.; Marsch-Martinez, N.; de Folter, S. Conserved and novel responses to cytokinin treatments during flower and fruit development in Brassica napus and Arabidopsis thaliana. *Sci Rep.* **2018**, *8*. [[CrossRef](#)]
36. Gerchikov, N.; Keren-Keiserman, A.; Perl-Treves, R.; Ginzberg, I. Wounding of melon fruits as a model system to study rind netting. *Sci. Hortic.* **2008**, *117*, 115–122. [[CrossRef](#)]
37. Henzell, R.F.; Briscoe, M.R.; Lauren, D.R. Evaluation of two plant growth regulators as chemical pruning agents for kiwifruit vines in summer. *N. Z. J. Exp. Agr.* **1986**, *14*, 199–203. [[CrossRef](#)]

38. Freiman, Z.E.; Rosianskey, Y.; Dasmohapatra, R.; Kamara, I.; Flaishman, M.A. The ambiguous ripening nature of the fig (*Ficus carica* L.) fruit: A gene-expression study of potential ripening regulators and ethylene-related genes. *J. Exp. Bot.* **2015**, *66*, 3309–3324. [[CrossRef](#)]
39. Ma, Y.; Shu, S.; Bai, S.; Tao, R.; Qian, M.; Teng, Y. Genome-wide survey and analysis of the TIFY gene family and its potential role in anthocyanin synthesis in Chinese sand pear (*Pyrus pyrifolia*). *Tree Genet. Genomes.* **2018**, *14*, 25. [[CrossRef](#)]
40. Giusti, M.M.; Wrolstad, R.E. Characterization and measurement of anthocyanins by UV-visible spectroscopy. In *Current Protocols in Food Analytical Chemistry*; Wrolstad, R.E., Acree, T.E., An, H., Decker, E.A., Penner, M.H., Reid, D.S., Schwartz, S.J., Shoemaker, C.F., et al., Eds.; John Wiley & Sons: New York, NY, USA, 2001; pp. F1.2.1–F1.2.13.
41. Wang, Z.; Du, H.; Zhai, R.; Song, L.; Ma, F.; Xu, L. Transcriptome analysis reveals candidate genes related to color fading of ‘Red Bartlett’ (*Pyrus communis* L.). *Front. Plant Sci.* **2017**, *8*, 455. [[CrossRef](#)]
42. Zhai, R.; Zhao, Y.; Wu, M.; Yang, J.; Li, X.; Liu, H.; Wu, T.; Liang, F.; Yang, C.; Wang, Z.; et al. The MYB transcription factor PbMYB12b positively regulates flavonol biosynthesis in pear fruit. *BMC Plant Biol.* **2019**, *19*, 85. [[CrossRef](#)] [[PubMed](#)]
43. Zhai, R.; Wang, Z.; Zhang, S.; Meng, G.; Xu, L. Two MYB transcription factors regulate flavonoid biosynthesis in pear fruit (*Pyrus bretschneideri* Rehd.). *J. Exp. Bot.* **2015**, *67*, 1275. [[CrossRef](#)] [[PubMed](#)]
44. An, J.; Yao, J.; Xu, R.; You, C.; Wang, X.; Hao, Y. An apple NAC transcription factor enhances salt stress tolerance by modulating the ethylene response. *Physiol. Plant.* **2018**, *164*, 279–289. [[CrossRef](#)] [[PubMed](#)]
45. Miao, L.; Zhang, Y.; Yang, X.; Xiao, J.; Zhang, H.; Zhang, Z.; Wang, Y.; Jiang, G. Colored light-quality selective plastic films affect anthocyanin content, enzyme activities, and the expression of flavonoid genes in strawberry (*Fragaria × ananassa*) fruit. *Food Chem.* **2016**, *207*, 93–100. [[CrossRef](#)]
46. Varasteh, F.; Arzani, K.; Barzegar, M.; Zamani, Z. Changes in anthocyanins in arils of chitosan-coated pomegranate (*Punica granatum* L. cv. Rabbab-e-Neyriz) fruit during cold storage. *Food Chem.* **2012**, *130*, 267–272. [[CrossRef](#)]
47. Qian, M.; Yu, B.; Li, X.; Sun, Y.; Zhang, D.; Teng, Y. Isolation and expression analysis of anthocyanin biosynthesis genes from the red Chinese sand pear, *Pyrus pyrifolia* Nakai cv. Mantianhong, in response to methyl jasmonate treatment and UV-B/VIS conditions. *Plant. Mol. Biol. Rep.* **2014**, *32*, 428–437. [[CrossRef](#)]
48. Zieslin, N.; Starkman, F.; Zamski, E. Growth of rose flower peduncles and effects of applied plant growth regulators. *Plant. Growth Regul.* **1989**, *8*, 65–76.
49. Nogueira, M.R.; Ferraz, M.V.; Bezerra, A.K.; Mazziniguades, R.B.; Costa, C.R.X.; De Almeida, L.C.; Pereira, S.T.; Pivetta, K.F. Indolbutyric acid and time of the year influence on rooting of chrysanthemum cuttings. *Am. J. Plant. Sci.* **2018**, *09*, 507–516. [[CrossRef](#)]
50. Yang, J.; Duan, G.; Li, C.; Liu, L.; Han, G.; Zhang, Y.; Wang, C. The crosstalks between jasmonic acid and other plant hormone signaling highlight the involvement of jasmonic acid as a core component in plant response to biotic and abiotic stresses. *Front. Plant. Sci.* **2019**, *10*, 1349. [[CrossRef](#)]
51. Suzuki, N. Hormone signaling pathways under stress combinations. *Plant. Signal. Behav.* **2016**, *11*, e1247139. [[CrossRef](#)]
52. Loreti, E.; Povero, G.; Novi, G.; Solfanelli, C.; Alpi, A.; Perata, P. Gibberellins, jasmonate and abscisic acid modulate the sucrose-induced expression of anthocyanin biosynthetic genes in *Arabidopsis*. *New Phytol.* **2008**, *179*, 1004–1016. [[CrossRef](#)] [[PubMed](#)]
53. Li, W.; Mao, J.; Yang, S.; Guo, Z.; Ma, Z.; Dawuda, M.M.; Zuo, C.; Chu, M.; Chen, B. Anthocyanin accumulation correlates with hormones in the fruit skin of ‘Red Delicious’ and its four generation bud sport mutants. *BMC Plant. Biol.* **2018**, *18*, 363. [[CrossRef](#)] [[PubMed](#)]
54. Jeong, S.T.; Goto-Yamamoto, N.; Kobayashi, S.; Esaka, M. Effects of plant hormones and shading on the accumulation of anthocyanins and the expression of anthocyanin biosynthetic genes in grape berry skins. *Plant. Sci.* **2004**, *167*, 247–252. [[CrossRef](#)]
55. Delker, C.; Stenzel, I.; Hause, B.; Miersch, O.; Feussner, I.; Wasternack, C. Jasmonate biosynthesis in *Arabidopsis thaliana*—enzymes, products, regulation. *Plant. Biol.* **2006**, *8*, 297–306. [[CrossRef](#)] [[PubMed](#)]
56. De Paepe, A.; Van Der Straeten, D. Ethylene biosynthesis and signaling: An overview. *Vitam. Horm.* **2005**, *72*, 399–430. [[PubMed](#)]
57. Müller, M.; Munné-bosch, S. Ethylene response factors: A key regulatory hub in hormone and stress signaling. *Plant. Physiol.* **2015**, *169*, 32–41. [[CrossRef](#)]

58. Stepanova, L.A.; Alonso, W.J. Ethylene signaling and response: Where different regulatory modules meet. *Curr. Opin. Plant. Biol.* **2009**, *12*, 548–555. [[CrossRef](#)]
59. Ouaked, F. A MAPK pathway mediates ethylene signaling in plants. *EMBO J.* **2003**, *22*, 1282–1288. [[CrossRef](#)]
60. McGrath, K.C.; Dombrecht, B.; Manners, J.M.; Schenk, P.M.; Edgar, C.I.; Maclean, D.J.; Wolf-Rüdiger, S.; Udvardi, M.K.; Kazan, K. Repressor- and activator-type ethylene response factors functioning in jasmonate signaling and disease resistance identified via a genome-wide screen of arabidopsis transcription factor gene expression. *Plant. Physiol.* **2005**, *139*, 949–959. [[CrossRef](#)]
61. Tan, X.; Fan, Z.; Shan, W.; Yin, X.; Kuang, J.; Lu, W.; Chen, J. Association of BrERF72 with methyl jasmonate-induced leaf senescence of Chinese flowering cabbage through activating JA biosynthesis-related genes. *Hortic. Res.* **2018**, *5*, 22. [[CrossRef](#)]
62. Zhang, G.; Chen, M.; Li, L.; Xu, Z.; Chen, X.; Guo, J.; Ma, Y. Overexpression of the soybean *GmERF3* gene, an AP2/ERF type transcription factor for increased tolerances to salt, drought, and diseases in transgenic tobacco. *J. Exp. Bot.* **2009**, *60*, 3781–3796. [[CrossRef](#)] [[PubMed](#)]
63. Zhang, H.; Huang, Z.; Xie, B.; Chen, Q.; Tian, X.; Zhang, X.; Zhang, H.; Lu, X.; Huang, D.; Huang, R. The ethylene-, jasmonate-, abscisic acid- and NaCl-responsive tomato transcription factor *JERF1* modulates expression of GCC box-containing genes and salt tolerance in tobacco. *Planta* **2004**, *220*, 262–270. [[CrossRef](#)] [[PubMed](#)]
64. Rouster, J.; Leah, R.; Mundy, J.; Cameron-Mills, V. Identification of a methyl jasmonate-responsive region in the promoter of a lipoxygenase 1 gene expressed in barley grain. *Plant. J.* **1997**, *11*, 513–523. [[CrossRef](#)] [[PubMed](#)]
65. Koyama, T.; Sato, F. The function of ethylene response factor genes in the light-induced anthocyanin production of *Arabidopsis thaliana* leaves. *Plant. Biotechnol.* **2018**, *35*, 87–91. [[CrossRef](#)] [[PubMed](#)]
66. Wang, Z.; Meng, D.; Wang, A.; Li, T.; Jiang, S.; Cong, P.; Li, T. The Methylation of the *PcMYB10* promoter is associated with green-skinned sport in Max Red Bartlett pear. *Plant. Physiol.* **2013**, *162*, 885–896. [[CrossRef](#)] [[PubMed](#)]
67. Feng, S.; Wang, Y.; Yang, S.; Xu, Y.; Chen, X. Anthocyanin biosynthesis in pears is regulated by a R2R3-MYB transcription factor *PyMYB10*. *Planta* **2010**, *232*, 245–255. [[CrossRef](#)]



© 2020 by the authors. Licensee MDPI, Basel, Switzerland. This article is an open access article distributed under the terms and conditions of the Creative Commons Attribution (CC BY) license (<http://creativecommons.org/licenses/by/4.0/>).